

VARIATIONS OF THE PARAMETERS OF BACKGROUND SEISMIC NOISE IN THE STAGE OF PREPARATION OF STRONG EARTHQUAKES IN THE VRANCEA REGION

E. Oynakov, I. Aleksandrova, D. Solakov

National Institute of Geophysics, Geodesy and Geography, Bulgarian Academy of Sciences, Acad. G. Bonchev Str., bl.3, Sofia 1113, Bulgaria, e-mail: i.alex@abv.bg

DOI: 10.34975/bgj-2019.42.2

Abstract. The Balkans, including Bulgaria, is one of the most seismogenic zones in Europe. The relatively small depth of the hypocentres of earthquakes - up to 60-70 km, could greatly increase the effects on the ground surface. In conditions of relatively high population density and high urban constructions, even a moderate magnitude earthquake could lead to increased unfavourable consequences - destruction and human losses.

The global impacts of atmospheric and oceanic processes, tidal deformations of the earth's crust, as well as the less well-studied processes in the Earth's crust, are associated with accumulation and slow dissipation of tectonic energy in the lithosphere. These processes are the „participants“ in the formation of the random process, where the traditional apparatus of spectral analysis is less effective.

The usage of fractal analysis for decipher the structure of seismic noise is a good enough alternative. Since the early 1990s, the method is used in both: turbulence analysis and in financial and medical time series studies.

The development of new methods for earthquake forecasting based on data from geophysical and, in particular, seismic monitoring, is one of the priority goals of Earth science. Seismic records of twenty-three Balkan Peninsula stations were analyzed, at distances of 1 to 500 km far from the earthquake on 23.09.2016, 27.12.2016 and 28.10.2018 with magnitude more 5.5 in seismic zone Vrancea. For the analysis, the Lubusin method was used for fractal analysis of scalar time series.

A scientific goal is to detect common signals ignoring the „individual“ behavior of the elements of the monitoring systems.

Key words: earthquake indicators, seismic noise, fractal analysis of seismic noise

Introduction

Microseismic oscillations in a wide frequency range are one of the most widespread objects of geophysical studies. This is due to their accessibility, the presence of numerous regional and global seismic networks, and the well-developed practice of seismic observations. Even an approximate review of the literature, devoted to analysis of microseisms, apparently cannot be made.

This is particularly true for the analysis of high frequency (HF) microseisms (from 0.01 to 100 Hz and higher, up to seismoacoustic waves). The widespread occurrence of HF microseismic observations is due to the relative simplicity and mobility of instrumentation, free from rigid requirements on long-term stability of sensors that can by no means be neglected in problems of low frequency (LF) geophysical monitoring. McNamara and Buland [2004] presented results of detailed research into microseismic background of natural and industrial origin in the frequency band 0.01–16 Hz, including the construction of estimators for the temporal (diurnal and seasonal) and spatial distribution of power spectrum properties. With an increase in the period of microseismic background oscillations studied, the role of atmospheric and oceanic waves, as main sources of microseisms, becomes predominant. Berger et al. [2004] presented a review of the use of IRIS broadband seismic stations for the study of background microseisms. Microseismic oscillations in the period range 5–40 s were studied by Stehly et al. [2006], who established their oceanic origin. Continuously observed microseismic oscillations at periods of 100–500s were examined in Friedrich et al., [1998]. These oscillations are generated both by weak earthquakes and by processes in the atmosphere, although the atmospheric effects are predominant.

The effect of atmospheric processes (movement of cyclones) and oceanic waves, generated by them, as well as the impact of the waves on the shelf and coasts, contributes most to the energy of the LF microseismic background.

The origin of an LF seismic hum with a predominant period of 4 min was studied in Rhie and Romanowicz [2004, 2006]. A significant correlation was established between the intensity of these oscillations and the oceans wave height, caused by storms, and it was shown that the hum intensity is independent of the Earth's seismic activity: the authors presented an example of a seismically quiet time interval (January 31– February 3, 2000) characterized, however, by anomalously high amplitudes of microseismic background in the vicinity of the 4-min period. As a possible mechanism of excitation of such oscillations, they proposed the perturbation of the gravitational field by high waves, resulting in the excitation of LF seismic waves on the seafloor. The main regions of excitation of these oscillations are suggested to be the northern Pacific Ocean in winter and the southern Atlantic Ocean in summer.

Low frequency oscillations of microseismic background and the Earth's gravitational field with periods of a few tens to a few hundreds of minutes arising, due to the lithosphere–atmosphere coupling, were considered in Linkov, [1987]. It is important that the source of such oscillations is supposedly slow wavelike deformations of the lithosphere.

The present paper generalizes the experience, accumulated in studies of microseismic background in the (LF) range of periods from 1 to 300 min, observed in time inter-

vals, preceding a few strong earthquakes [Oynakov, Aleksandrova 2019; Oynakov E., et al. 2019].

This frequency range is the least studied and occupies an intermediate position between LF seismology and investigations of slow geophysical processes, such as gravity field variations, crustal strain and tilt variations, and so on. The range includes various modes of the Earth's free oscillations, excited by strong earthquakes; however, in the present paper, the main attention is given to the background behavior of microseisms. Note that this background contains continuous arrivals from near weak and far strong and moderate earthquakes.

In this paper, the main emphasis is placed on the study of synchronization effects, appearing in a joint multidimensional analysis of information from several stations. The synchronization effects of the microseismic background are also examined, as a means for detecting new precursors of strong earthquakes.

Method and Theory

Let F be some random fluctuations in the time interval $[t-\delta/2, t+\delta/2]$ (Figure 1) with duration δ and the reach of the random process for this interval - $\mu(t, \delta)$ (difference between the maximum and minimum amplitude values) and calculate the mean value of its power degree q : $M(\delta, q) = [(\mu_x(t, \delta))^q]$.

A random signal is scale-invariant [Taqqu, 1988] if $M(\delta, q) \sim \delta^{(q)}$ when $\delta \rightarrow 0$, that is, the following limit exists:

$$\rho(q) = \lim_{\delta \rightarrow 0} \left(\frac{\ln M(\delta, q)}{\ln(\delta)} \right). \quad (1)$$

If $\rho(q)$ is a linear function $\rho(q) = Hq$, where $H = \text{const}$, $0 < H < 1$, the process is called monofractal. In the case where $\rho(q)$ is a nonlinear concave function of q , the signal is called multifractal. To estimate the value of $\rho(q)$ using a finite sample $x(t)$, $t = 0, 1, \dots, N-1$ we used the method, which is based on the approach of detrended fluctuation analysis (DFA) [Kantelhardt et al., 2002]. Let us split the entire time series into non-overlapping intervals of length s :

$$\mathbf{I}_k^{(s)} = \left\{ t : 1 + (k-1)s \leq t \leq ks, k = 1, \dots, \left[\frac{N}{s} \right] \right\} \quad (2)$$

and let

$$\mathbf{y}_k^{(s)}(t) = \mathbf{x}((k-1)s + t), t = 1, \dots, s \quad (3)$$

be a part of the signal $x(t)$, corresponding to interval $\mathbf{I}_k^{(s)}$. Let $\mathbf{p}_k^{(s,m)}(t)$ be a polynomial of the order m , best fitted to the signal $\mathbf{y}_k^{(s)}(t)$. Let us consider the deflections from the local trend:

$$\Delta y_k^{(s,m)}(t) = y_k^{(s)}(t) - p_k^{(s,m)}(t), \quad t = 1, \dots, s \quad (4)$$

and calculate the values

$$Z^{(m)}(q, s) = \left(\frac{\left(\sum_{k=1}^{N/s} \left(\max_{1 \leq t \leq s} \Delta y_k^{(s,m)} - \min_{1 \leq t \leq s} \Delta y_k^{(s,m)}(t)^q \right) \right)^{\frac{1}{q}}}{\frac{N}{s}} \right) \quad (5)$$

that can be regarded as the estimate of $(M(\delta_s, q))^{\frac{1}{q}}$. Let us define the function $h(q)$ as a coefficient of linear regression between $\ln(Z^{(m)}(q, s))$ and $\ln(s)$: $Z^{(m)}(q, s) \sim s^{h(q)}$ fitted for scales range $s_{min} \leq s \leq s_{max}$. It is evident that $(q) = qh(q)$ and, for a monofractal signal, $h(q) = H = const$. The multifractal singularity spectrum $F(\alpha)$ is equal to the fractal dimensionality of the set of time moments t for which the Hölder – Lipschitz exponent is equal to α i.e. for which $|x(t + \delta) - x(t)| \sim |\delta|^\alpha, \delta \rightarrow 0$ [Feder, 1988]. The singularity spectrum can be estimated using the standard multifractal formalism, which consists in calculating the Gibbs sum: multifractal formalism, which consists in calculating the Gibbs sum:

$$W(q, s) = \sum_{k=1}^{N/s} \left(\max_{1 \leq t \leq s} \Delta y_k^{(s,m)}(t) - \min_{1 \leq t \leq s} \Delta y_k^{(s,m)}(t) \right)^q \quad (6)$$

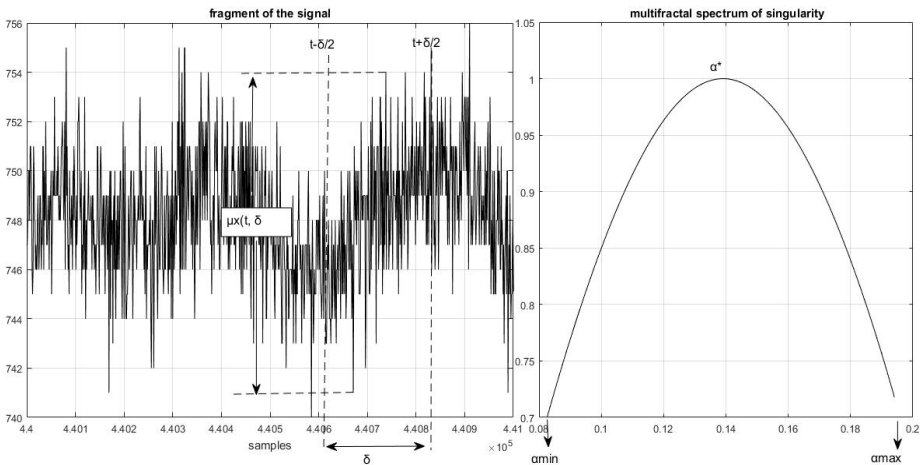


Fig. 1. Illustration of the multifractal spectrum of the singularity, where: $F(\alpha)$ – the multifractal spectrum of the singularity or fractal dimension of the set of times t ; $\Delta\alpha$ – width of the carrier of $F(\alpha)$; α^* – a general exponent Hurst

and in estimating the mass exponent $\tau(q)$ from the condition $W(q, s) \sim s^{\tau(q)}$. From (6) it follows that $\tau(q) = \rho(q) - 1 = qh(q) - 1$. In the next step, the spectrum $F(\alpha)$ is calculated with the Legendre transform:

$$F(\alpha) = \max_q \{ \min(\alpha q - \tau(q)), 0 \}. \quad (7)$$

If the singularity spectrum $F(\alpha)$ is estimated in a moving window, its evolution can give useful information on the variations in the structure of the “chaotic” pulsations of the series. In particular, the position and width of the support of the spectrum $F(\alpha)$, i.e., the values α_{\min} , α_{\max} , $\Delta\alpha = \alpha_{\max} - \alpha_{\min}$ and α^* , such that $F(\alpha^*) = \max_{\alpha} F(\alpha)$, are characteristics of the noisy signal. The value α^* can be called a generalized Hurst exponent and it gives the most typical value of Lipschitz-Holder exponent. Parameter $\Delta\alpha$, singularity spectrum support width, could be regarded as a measure of variety of stochastic behavior. In the case of a monofractal signal, the quantity $\Delta\alpha$ should vanish and $\alpha^* = H$. Usually $F(\alpha^*) = 1$, but there exist time windows for which $F(\alpha^*) < 1$. Estimates of minimum Hölder-Lipschitz exponent $\min \alpha$ are mainly positive. Nevertheless negative values of $\min \alpha$ are quite possible as well for time fragments which are characterized by high-amplitudes spikes and steps.

Used data

This article explores the time interval of 01.08.2016. - 30.12.2016, involving three seismic events with $M_w > 5.5$:

- the earthquake of 23.09.2016; $T_0=11:11:20$ GMT; with coordinates 45.71°N / 26.62°E; $M_w = 5.7$; $h = 92$ km;
- the Vrancea earthquake on 27.12.2016; $T_0=11:20:56.3$ GMT; with coordinates 45.72°N / 26.61°E; $M_w = 5.6$; $h = 91$ km;
- the Vrancea earthquake on 28.10.2018; $T_0= 00:38:15$ GMT; with coordinates 45.7°N / 26.4°E; $M_w=5.5$; $h = 150$ km.

For the study, vertical component records (Z) of 23 seismic stations (Table 1), with records of 100 reports per second (i.e., 8 640 000 reports for 24 hours) are used. In order to obtain 1/2-minute low-frequency noise time series, the average values of the original recordings at successive time intervals of 3000 reports calculated for each station — 1/2 minute time series are obtained for all 23 stations.

Eight of the seismic stations - PLOR, PLOR1, PLOR2, PLOR3, PLOR4, PLOR5, PLOR6 and PLOR7 (Local Ploeschina network), located in the epicentral region (average 20 km from the epicentres of the two earthquakes) of the Vrancea seismic zone, VRI and DRGR stations are located at distances of 30 and 450 km respectively from the earthquake epicentres. All ten listed seismic stations are part of the seismic network of Romania. The seismic stations PRD, AVR, BOZ, DOB, NEF, and ROIA, are part of the Prova-

Table 1. Seismic stations used in the study. The last 3 columns represent the time intervals and the number of 24-hour seismic records, used in the research.

Seismic stations	Digitizer	Latitude (°N)	Longitude (°E)	Sensors	Period 01.08.16 – 23.09.16 Number of 24 hour records	Period 24.09.16 – 30.12.16 Number of 24 hour records	Period 06.09.18 – 30.10.18 Number of 24 hour records
AVR	DAS 9AF3	43,1178	27,6685	GEOPHON	54	98	53
BOZ	DAS 98B6	43,1044	27,4786	GEOPHON	54	98	53
DOB	DAS 9C9D	43,1790	27,4628	GEOPHON	54	98	53
PRD	DAS 990A	43,1602	27,4099	GURALP	54	98	53
NEF	DAS 986E	43,2644	27,2753	S13	54	98	53
ROIA	DAS 9913	43,0934	27,3778	GEOPHON	54	98	53
PSN	DAS A646	43,6376	28,1359	KS2000/60s	54	98	53
PVL	DAS 990C	43,1227	25,1732	CMG 3ESPC/120	54	98	53
MPE	DAS A625	43,3560	23,7401	S13	54	98	53
SZH	DAS 9901	43,2653	25,9762	CMG 3ESPC/120	54	98	53
ORH	DAS9D18	43,7263	23,9664	S13	54	98	53
VLD	DAS9B2E	43,6899	23,4356	S13	54	98	53
VRI	Altus-K2	45,8665	26,2764	CMG3ESP	54	98	53
DRGR	Altus-K2	46,7917	22,7111	KS54000	54	98	53
PLOR	Q330	26,6498	45,8512	STS2	54	98	53
PLOR1	Q330	45,8520	26,6466	CMG-40T	54	98	53
PLOR2	Q330	45,8502	26,6437	CMG-40T	54	98	53
PLOR3	Q330	45,8539	26,6454	CMG-40T	54	98	53
PLOR4	Q330	45,8512	26,6498	CMG-40T	54	98	53
PLOR5	Q330	45,8455	26,6635	CMG-40T	54	98	53
PLOR6	Q330	45,8419	26,6415	CMG-40T	54	98	53
PLOR7	Q330	45,8603	26,6405	CMG-40T	54	98	53
					1242	2254	1219

dia Local Seismic Network (LSN-Provadia). They are at an average distance of 400 km from the epicenters of the two earthquakes, the PSN, PVL, MPE, SZH, ORH and VLD seismic stations are part of the seismic network of Bulgaria and located at approximately 370 km, 430 km, 470 km, 380 km, 420 km and 460 km from the epicenters, respectively.

With the used methodology, three informative fractal statistics are estimated at consecutive time intervals of 2880 report (1 day) for 1/2-minute time series for each station. The estimation of the values of the noise statistics is made after the separation of the low-frequency trend using an 8th-order polynomial. Trend filtering is required to eliminate the effects of tidal and temperature deformations of the Earth's crust in the seismic noise variations and also represents a necessary procedure for studying the noise's statistical characteristics. The usage of an orthogonal polynomial enables the stability of the

trend evaluations at the reading points. In this case, the order of the polynomial (8th) was chosen as the smallest one after numerical experiments, thus allowing the elimination of the day-to-day variations for the intervals of one-day duration (Lyubushin, A. A. 2007). The question of the regularity of the transition in such a low-frequency domain of seismic signal recordings naturally arises.

It should be noted that the development of seismological apparatus did not consider its use for continuous seismic recording over a more extensive frequency range beyond the earthquake signal frequencies, and is not assumed that seismic sensors could also be used as the usual inclinometer, i.e., to register the change of signal in the tidal band frequencies. Following numerical experiments (Lyubushin AA, 2008), we believe that in solving geophysical monitoring tasks and investigating earthquake preparation processes, there is a theoretical possibility for broader use of seismological equipment that exceeds the formal operating frequency limitations, which is traditionally used to study individual earthquakes. Fig. 2 shows the graphs, illustrating this consideration. Continuous, uninterrupted seismic noise recordings of the taken eight stations and a 1-hour discretization step are made. From the initial recordings at a sampling rate of 100 Hz, the average value was calculated at consecutive time intervals with a length of 360,000 reports, which is 1 hour. In this way, the traditional for gravimetry frequency range is provided. If adhering to the traditional view of such a procedure, the transition to an hourly discretization step seems unacceptable.

Moreover, if we look at the power spectra of the temporal variations of the seismic noise (Oynakov E. et al.2019), recorded with the instrumentation used (Table 1), we see the manifestation of tidal 12 and 24-hour spectral extremum, even separation of different tidal harmonics at sufficient length of time series. This example shows that the signal, recorded with modern seismometers, contains low-frequency components, significantly exceeding the formal limits, specified in their technical passports by the manufacturer. It is these undocumented and poorly understood capabilities of seismometers that could be used in this study.

It should also be pointed out that all of the used noise statistics are dimensionless and do not depend on the scale of the output data. That significantly reduces their dependence on the fact that different seismometers have been installed at the seismic stations.

Results - Hurst exponent

The interest towards the positive value of the Hurst exponent estimate ($H > 0$) is related to the fact that for self-similar processes it is in the interval $0 < H < 1$ (Kantelhardt, Jan W., et al., 2002). Therefore, $H(\tau) > 0$ represents a sign of self-similar fractal behavior of low-frequency seismic noise, indirectly. It is of our interest to separate those time windows, as for all simultaneously analyzed processes, the Hurst exponent is positive, which is a sign of low-frequency synchronization – a possible sign of a future earthquake.

The results obtained show that 2 to 4 days before the earthquake on October 28, 2018, with $M_w = 5.5$ and 2 to 3 days before the earthquake on October 18.2018 with $M_W = 3.7$, the Hurst index has a high value (Fig. 2).

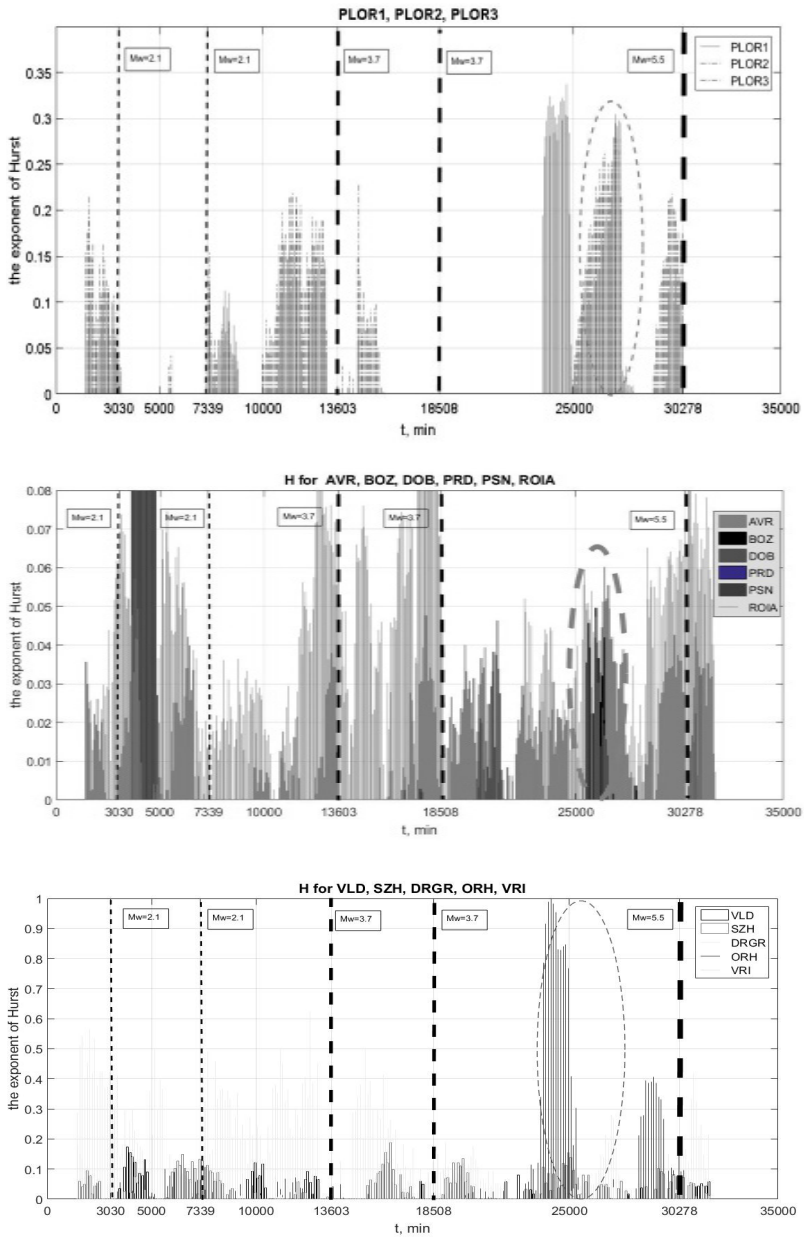


Fig. 2. Graphs of the change in the Hurst (H) metric for different stations combination, calculated in a time window 1 day and 1 hour displacement; the red dotted line shows the moment of the earthquake - 28.10.2018 (Vrancea, $T_0=00:38:15$; $45.7 / 26.4$; $M = 5.5$) and the earthquakes that occurred in the analysed area.

To verify that before earthquakes of magnitude higher than $M_w = 5.5$ in the seismogenic zone of Vrancea, the Hurst (H) exponent increases, both significant earthquakes in 2016 were examined. Fig. 3 shows a graph of the synchronous maximum of H in the period 01.08-30.12.2016, for the stations of the Local Ploeschina network. From the graph, we can summarize that 12 days before the earthquake on September 23, 2016, and 8 days before the earthquake of December 27, 2016, the values of H have increased.

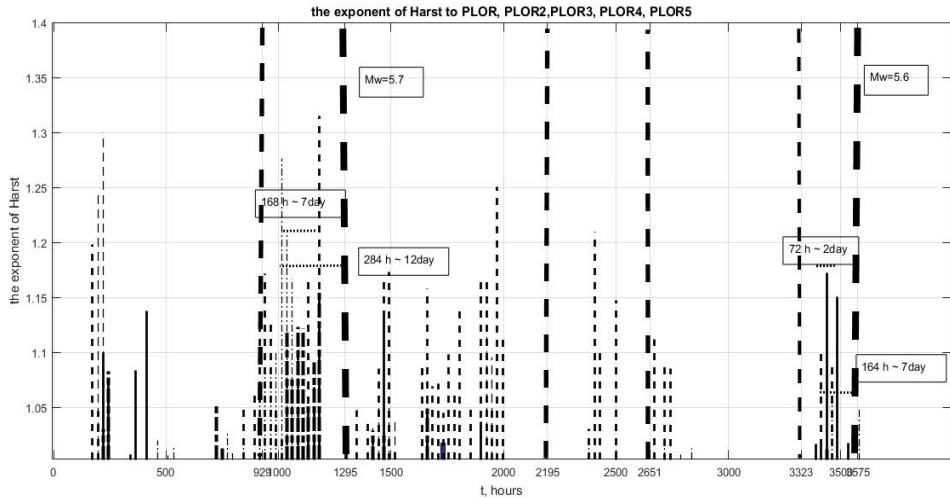


Fig. 3. Graph of the change of $H > 0$ for PLOR, PLOR2, PLOR3, PLOR4, PLOR5 stations; the red dashed lines show the moments of the earthquakes that occurred in the analysed area in the period 01.08-30.12.2016 – 08.09.2016 ($M_w = 4.1$); 09.23.2016 ($M = 5.7$); 10.31.2016 ($M_w = 4$); 11.19.2016 ($M_w = 4.1$); 11.30.2016 ($M_w = 3.5$); 12.17.2016 ($M_w = 3.9$) and 12.27.2016 (Vrancea, $T_0=00:38:15$; $45.7N$, $26.4E$; $M_w = 5.6$). The text boxes show the time from H maxima to the earthquake moments in minutes and days.

Fig. 4 presents in detail the graphs of the Hurst exponent evaluations for DRG, MPEP, VRI stations in the period 23.09-30.12.2016 before the earthquake of December 27, 2016 (Vrancea, $M_w = 5.6$). The zero of the time axis corresponds to $T_0 = 00:00:00$ (GMT) on 23.09.2016. It can be noted that the maximum of the Hurst exponent is present not only before the earthquake of 27.12.2016 but also ~ 9 days before the earthquake of 17.12.2016, $T_0=11: 16: 05$ (GMT) with coordinates $45.5^\circ N$, $26.47^\circ E$ and $M_w = 3.8$.

Fig. 5 shows in detail the graphs of the Hurst indicator evaluations for stations AVR, DRGR, MPEP, NEF, ORH, PRD, PSN, ROIA, SZH, VRI before the earthquake of 23.09.2016. (Vrancea, $M_w = 5.7$). The zero of the time axis corresponds to 23.08.2016, 00h00m (GMT). Three more seismic events occur in the analysed period (01.09.2016; $T_0=07: 49: 21$; $45.67^\circ N$, $26.33^\circ E$ ($M_w = 3.9$); 08.09.16; $T_0= 17: 03: 02$; $45.67^\circ N$, $26.53^\circ E$

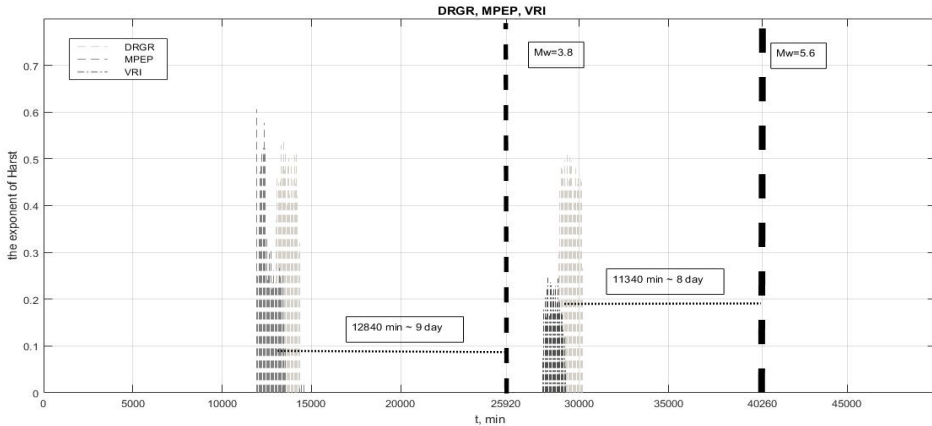


Fig. 4. Graph of the change of $H > 0$ for DRGR, MPEP, VRI stations in the period 24.09-30.12.2016. The red dashed lines show the moment of the earthquakes that occurred in the analysed area - 17.12.16; $T_0 = 11: 16: 05$; 45.50°N , 26.47°E ($M_w = 3.9$); and 27.12.2016 (Vrancea, $T_0 = 12:38:15$; 45.7°N , 26.4°E ; $M_w = 5.5$). The text boxes show the time from H maxima to the earthquake moments in minutes and days.

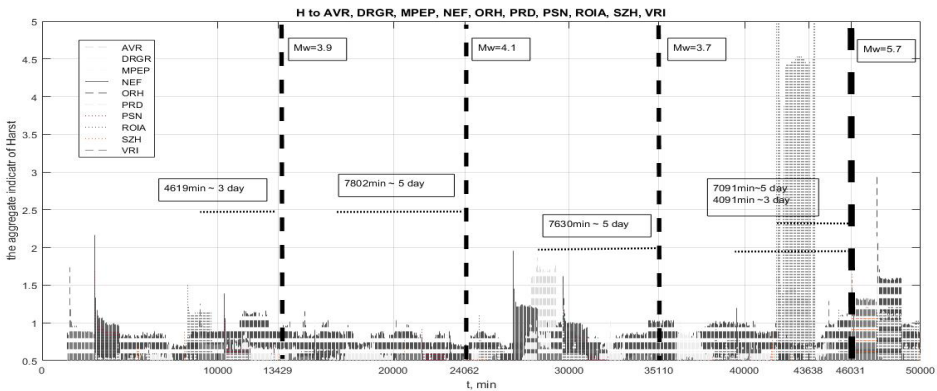


Fig. 5. Graph of the change of $H > 0$ for AVRR, DRGR, MPEP, NEF, ORH, PRD, PSN, ROIA, SZH and VRI stations in the period 23.08-23.09.2016. The red dashed lines indicate the time of the earthquakes that occurred in the analysed area - 01.09.2016; $T_0 = 07: 49: 21$ (GMT); 45.67°N , 26.33°E ($M_w = 3.9$); 08.09.2016; $T_0 = 17: 03: 02$; 45.67°N , 26.53°E ($M_w = 4.1$); 16.09.2016; $T_0 = 09: 10: 57$; 45.65°N , 26.59°E ($M_w = 3.7$) and 23.09.2016 (Vrancea, $T_0 = 23:11:20$; 45.71°N , 26.62°E ; $M_w = 5.7$). The text boxes show the time from H maxima to the earthquake moments in minutes and days.

($M_w = 4.1$); 16.09.2016; $T_0 = 09: 10: 57$; 45.65°N , 26.59°E ($M_w = 3.7$)) and it can be noted that 3 to 5 days before each event there is a synchronous maximum of H for all stations. The figure also shows that the Hurst indicator for all stations is $H > 0$.

Results- Singularity spectrum width

The parameter $\Delta\alpha = \alpha_{max} - \alpha_{min}$ (Feder E., 1991), also called the width of the singularity spectrum, represents one of the important multifractal characteristics and assessments for the variety of random signal behavior. The statistically significant decrease in the average value of $\Delta\alpha$ reflects the decrease in the degrees of system's freedom, generating a signal and thus enables the determination of the time of preparation of an earthquake.

Fig. 6 presents a graph of the overall assessment of the parameter $\Delta\alpha$ for all stations on the PLOR LAN (i.e., the average value of $\Delta\alpha$). For each station, $\Delta\alpha$ is calculated in consecutive non-intersecting windows with a length of 24 hours and a shift of 1 hour over the entire time interval (06.09-30.10.2018, 52 days), after which the average value for the local area network is obtained. One feature of the smoothed $\Delta\alpha$ schedule are the minimums 4 days before the earthquakes on 28.10.2018, respectively, which, as we have indicated above, measures the number of hidden degrees of freedom of the stochastic systems. The other earthquakes in the analyzed time interval are preceded by a minimum of the width index of the singularity spectrum from 1 to 4 days.

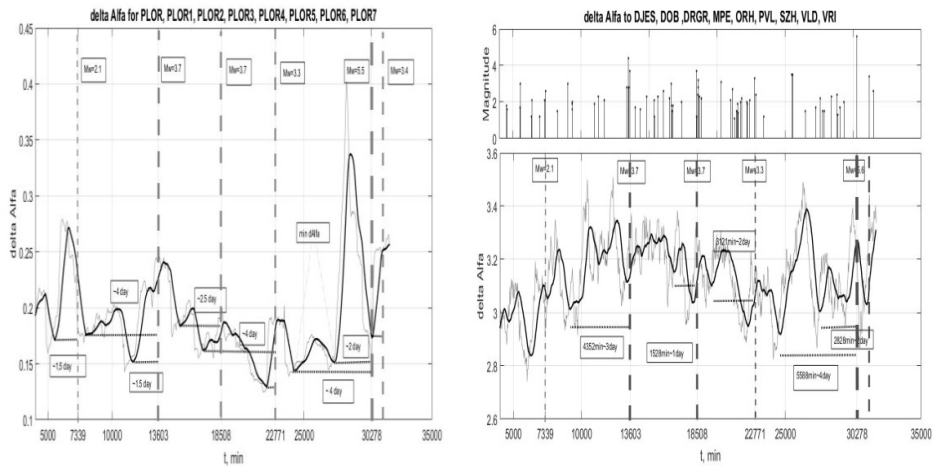


Fig. 6. Diagram of the mean values of parameter $\Delta\alpha$, for stations - DOB, DRGR, MPE, ORH, PVL, SZH, VLD, VRI, between 06.09 and 28.10.2018. Combined with the graphs of all the earthquakes that occurred in the Balkan Peninsula in the period 06.10 - 28.10.2018.

Fig. 7 presents a graph of the overall assessment of the parameter $\Delta\alpha$ for all stations on the PLOR LAN (i.e., the average value of $\Delta\alpha$). For each station, $\Delta\alpha$ is calculated in consecutive non-intersecting windows with a length of 24 hours and a shift of 1 hour over the entire time interval (01.08-30.12.2016, 22 days), after which the average value for the local area network is obtained. One feature of the smoothed $\Delta\alpha$ schedule are the minimums in the 59400 and 199700 minutes, 13 and 10 days before the earthquakes on 23.09.2016 and 27.12.2016. The other earthquakes in the analyzed time interval are

preceded by a minimum of the width index of the singularity spectrum from 6 to 7 days. We may also note a large minimum of $\Delta\alpha$ at 95040 minutes, which precedes the earthquakes at 109796, 119710, and 131759 minutes, and can be assumed to be related to them.

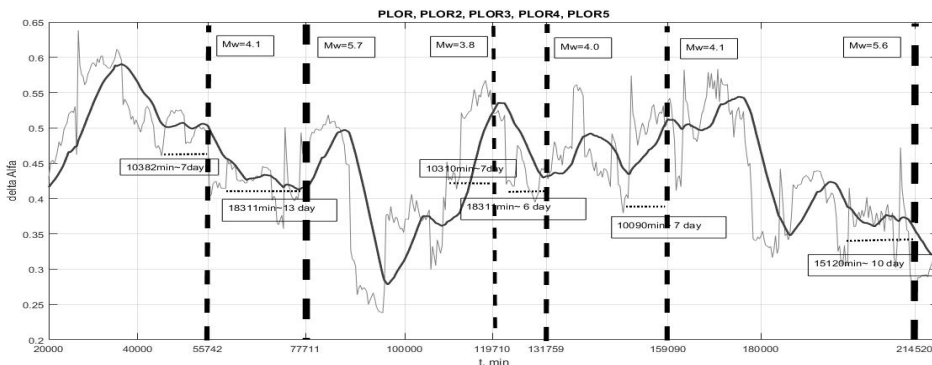


Fig. 7. Graph of the average values of the parameter $\Delta\alpha$, for stations from the local area network Ploeschina. The dashed line indicates all earthquakes, occurrences in the analyzed area for the period. The beginning of the abscissa is 06.10.2018 – 00:00 hours (GMT).

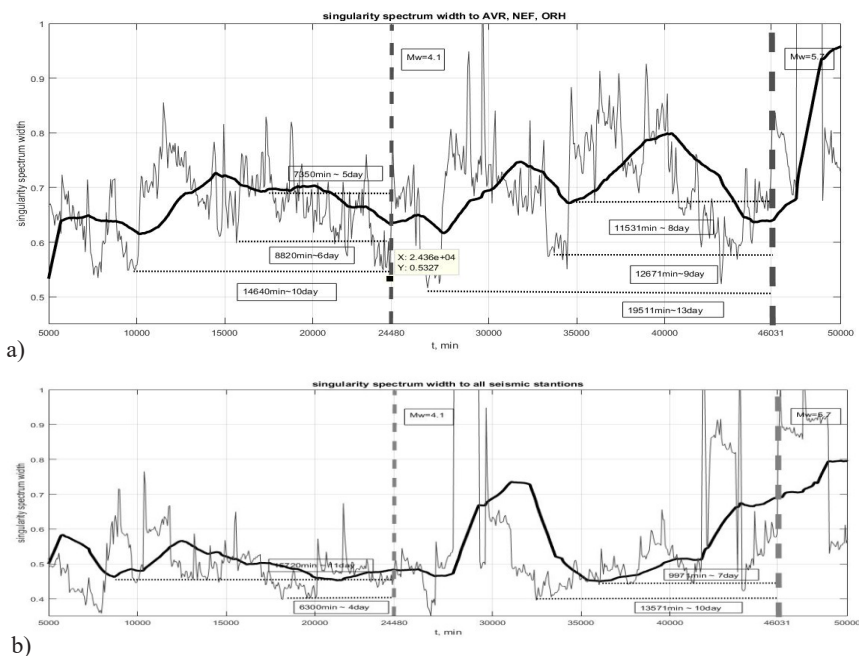


Fig. 8. Graph of the average values of the parameter $\Delta\alpha$ **a)** for stations - AVR, NEF, ORH in the interval 01.08 to 24.09.2016. **b)** for stations - DRGR, PRD, PSN, VRI in the interval 01.08 to 24.09.2016. The red dashed lines mark the moments of the earthquakes

Fig. 8 a), b) shows the evolution of the width parameter of the spectrum of singularity $\Delta\alpha$ for the interval 23.08-23.09.2016 for different station combinations. The $\Delta\alpha$ parameter for each station is calculated for the same length of the time window (24 hours = 2880 reports) and the same displacement (1 hour = 120 reports). Minima of $\Delta\alpha$ can be determined both 6-7 days before the earthquake with $M_w = 5.7$ (23.09.2016) and 3-5 days before the earthquakes, falling within the studied time interval. It should be added that a study on the evolution of the width of the spectrum of singularity before the earthquake of December 27, 2016, was also conducted. ($M_w = 5.6$) in the period 23.08-23.09.16 and the results are identical, i.e., 6-10 days before the earthquake, there is a minimum of $\Delta\alpha$, and 3-4 days before the weaker earthquakes, falling within the analyzed interval.

Results - Spectral Coherence Assessment

For assessing the synchronization effects of the results, measuring of the low-frequency microseismic background for several seismic stations, is used the spectral measure of coherence, proposed by Lyubushin (1998). It is constructed as a module of the product of the component canonical coherence.

$$\lambda(\tau, \omega) = \prod_{j=1}^m |v_j(\tau, \omega)|,$$

where $m \geq 2$ is the total number of jointly analyzed time series (the dimension of the multidimensional time series), ω is the frequency, τ is the time coordinate of the right edge of the scandent time window, $v_j(\tau, \omega)$ is the canonical coherence of the j th scalar time row that describes the relationship between that row and the other ones. The inequality $0 \leq |v_j(\tau, \omega)| \leq 1$ is satisfied. The closer the value of $|v_j(\tau, \omega)|$ is to one, the higher linearly are connected the variations of the j th order of frequency ω in the time window with coordinate τ to the similar variations in other lines studied. Accordingly, measure $0 \leq \lambda(\tau, \omega) \leq 1$ describes the effect of the overall coherent (synchronous, collective) behavior of all signals.

Fig. 9 a) shows the behaviour of the spectral measure of coherent behaviour $\lambda(\tau, \omega)$ of the seismic signal for stations PLOR1-PLOR7, in a time window 20160 half minute reports (7 days) with 720 reports (6 hours) shift for the time interval 06.09.2018 – 30.10.2018 (the abscissa timestamps indicate the right end of the time window). From the result we can conclude that the signal synchronization of all stations has a maximum of all frequencies in 24000 minutes, which is ~ 5 days before the earthquake which is in 30278 minutes (28.10.18, $M_w = 5.5$) and b) shows the behaviour of the spectral measure of coherent behaviour $\lambda(\tau, \omega)$ of the seismic signal for stations MPE; NEF; ORH; PSN; PVL; ROIA; SZH ; VLD. From the result we can conclude that the signal synchronization of all stations has a maximum from 19000 to 21000 minutes, which is ~ 9 to 7 days before the earthquake.

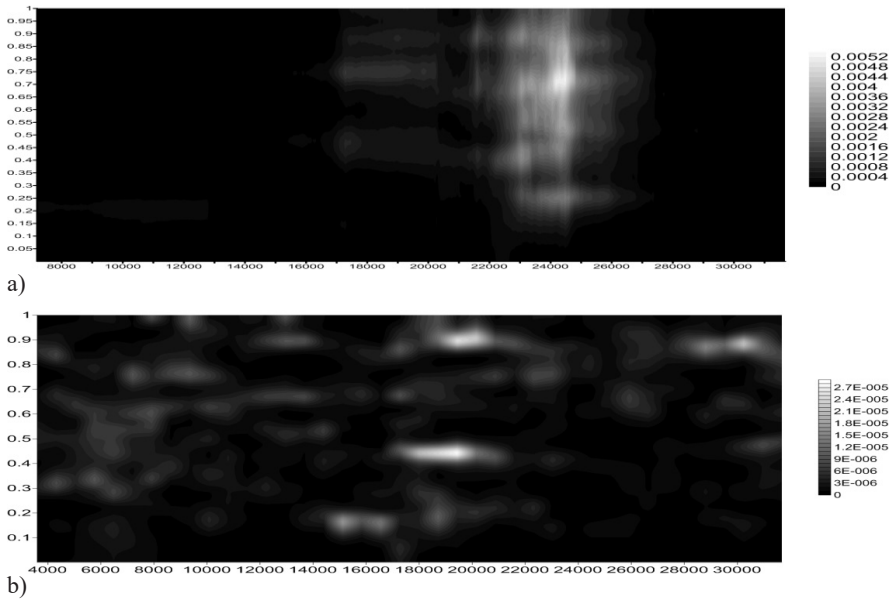


Fig. 9. Frequency-time diagram of the evolution of $\lambda(\tau, \omega)$ (spectral measure of coherent behaviour) for PLOR1-PLOR7 stations **a)**; end MPE; NEF; ORH; PSN; PVL; ROIA; SZH; VLD stations **b)**.

Fig. 10 shows the behaviour of the spectral measure of coherent behaviour $\lambda(\tau, \omega)$ of the seismic signal for stations PLOR1-PLOR7, in a time window 20160 half minute reports (7 days) with 720 reports (6 hours) shift for the time interval 01.08.2016 – 30.12.2016 (the abscissa timestamps indicate the right end of the time window). From the result we can conclude that the signal synchronization of all stations has a maximum of all frequencies in 30000 minutes, which is ~ 40 days before the earthquake which is in 77711 minutes (23.09.16, $M_w = 5.7$) and maximum in 14000 minutes - ~ 50 days before the earthquake in 214520 minutes (December 27, 2016, $M_w = 5.6$).

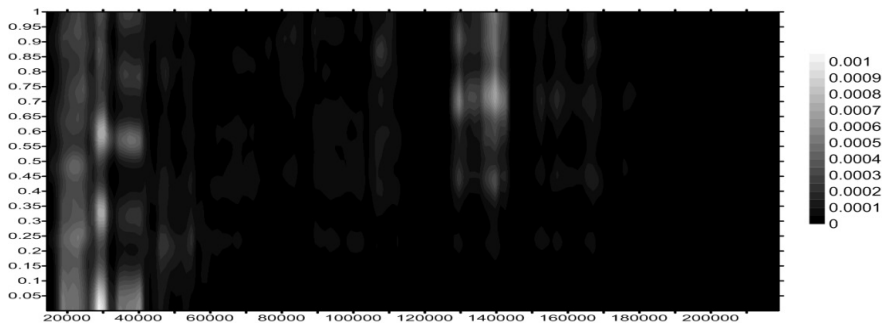


Fig. 10. Frequency-time diagram of the behavior of $\lambda(\tau, \omega)$ for PLOR1-PLOR7 stations. The beginning of the time axis corresponds to 00:00 (GMT) on 01.08.2016 (analyzed time interval from 01.08 to 30.12.2016)

Fig. 11 shows the behaviour of the spectral measure of coherent behaviour $\lambda(\tau, \omega)$ of the seismic signal for; MPE; NEF; ORH; PSN; PRD; ROIA; SZH; VLD; VRI stations, in time window 20160 half minute reports (7 days) with 720 reports (6 hours) shift for the time interval 23.09 - 30.12.2016 (abscissa timestamps indicate the right end of the time window). The signal synchronizations of all stations start from 20000 minutes and reach a maximum of 24000 minutes, which is ~ 15 days before the earthquake on December 27, 2016 ($M_w = 5.6$).

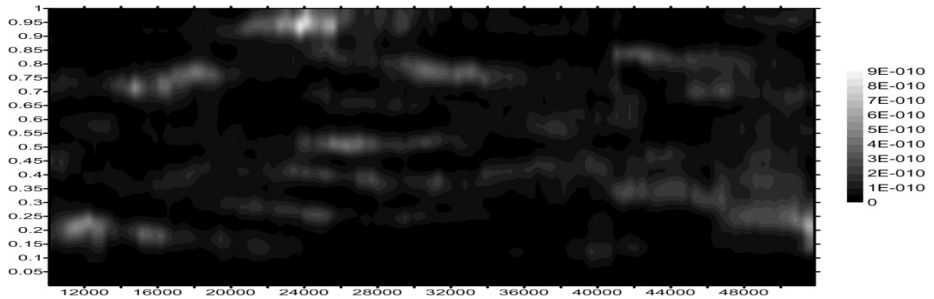


Fig. 11. Frequency-time diagram of the behavior of $\lambda(\tau, \omega)$ for MPE; NEF; ORH; PSN; PRD; ROIA; SZH; VLD; VRI stations, for the time interval 23.09.-30.12.2016. The moment of the earthquake of 27.12.2016 shown with an arrow.

Fig. 12 shows the behaviour of the spectral measure of coherent behaviour $\lambda(\tau, \omega)$ of the seismic signal for MPE; NEF; ORH; PSN; PRD; ROIA; SZH; VLD; VRI stations, in time window 20160 half minute reports (7 days) with 720 reports (6 hours) shift for the interval time 23.08 - 23.09.2016 (abscissa timestamps indicate the right end of the time window). The signal synchronizations of all stations start from 30,000 minutes and reach a maximum of 36,000 minutes, which is ~ 6 days before the earthquake on September 23, 2016 ($M_w = 5.7$).

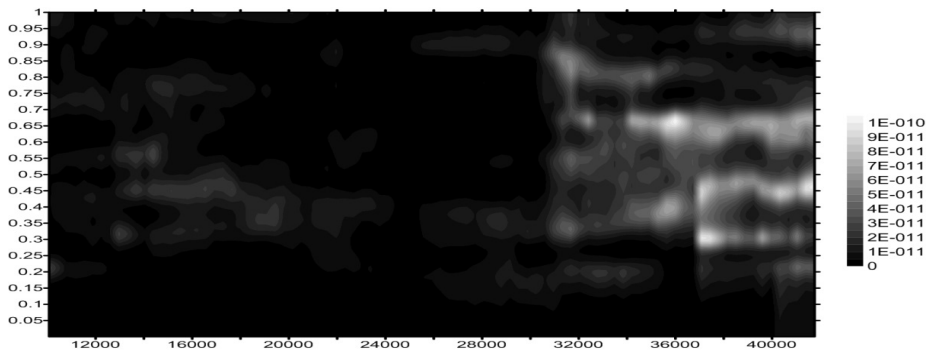


Fig. 12. Frequency-time diagram of the behavior of $\lambda(\tau, \omega)$ for MPE; NEF; ORH; PSN; PRD; ROIA; SZH; VLD; VRI stations, for the time interval 23.08.-23.09.2016. The moment of the 23.09.2016 earthquake is shown above with an arrow.

Conclusions

The study of the Hurst exponent shows that it increases about 7-8 days before earthquakes with $M_w > 5.5$. High H values were indicated 3 to 5 days before other smaller magnitude seismic events ($3.5 \leq M_w \leq 5$).

The analysis of the development of the width of the spectrum of singularity $\Delta\alpha$ shows that earthquakes with $M_w > 5.5$ in the analyzed time interval are preceded by minimums from 10 to 13 days and minimums of 2 to 7 days before earthquakes with smaller magnitude ($3.5 \leq M_w \leq 5$).

The spectral time diagram of the spectral measure of coherent behaviour of the seismic signal for epicentral stations, estimated in a time window of 10080 minutes (7 days), with a 360 minutes (6 hours) shift, for the time interval 01.08 - 30.12.2016, shows synchronization of the stations from 40 to 50 days prior to the earthquakes in Vrancea with $M_w > 5.5$. For stations at a greater distance – from 6 to 15 days before the earthquakes (time window 2880 reports, 120 reports shift).

We can conclude that the analysis of the fractal and multifractal parameters of the microseismic field in the minute time range of discretization can provide valuable information about the process of earthquake preparation and the effects, leading to the accumulation of stress in the lithosphere.

Acknowledgements.

This study has been carried out within the framework of the National Scientific Program “Young Scientists and Postdoctoral Fellows”, approved by Council of Ministers Decision No 11 / 17.08.2018 and supported by the Ministry of Education and Science (MES) of Bulgaria and of the National Science Program “Environmental Protection and Reduction of Risks of Adverse Events and Natural Disasters”, approved by the Resolution of the Council of Ministers № 577/17.08.2018 and supported by the Ministry of Education and Science (MES) of Bulgaria (Agreement № ДЮ-230/06-12-2018).

References

- Berger J., Davis P., Ekström G. Ambient earth noise: a survey of the global seismographic network //Journal of Geophysical Research: Solid Earth. – 2004. – T. 109. – №. B11
- Feder E. Fractals. - M.: Mir, 1991. –254 p.(Ru)
- Friedrich R., Zeller J., Peinke J. A note on three-point statistics of velocity increments in turbulence //EPL (Europhysics Letters). – 1998. – T. 41. – №. 2. – C. 153
- Kantelhardt, Jan W., et al. „Multifractal detrended fluctuation analysis of nonstationary time series.“ Physica A: Statistical Mechanics and its Applications 316.1-4 (2002): 87-114
- McNamara D. E., Buland R. P. Ambient noise levels in the continental United States //Bulletin of the seismological society of America. – 2004. – T. 94. – №. 4. – C. 1517-1527
- Lyubushin A. A. Analysis of canonical coherences in the problems of geophysical monitoring // IZVESTIIA PHYSICS OF THE SOLID EARTH C/C OF FIZIKA ZEMLI-ROSSIISKAIA AKADEMIIA NAUK. – 1998. – T. 34. – C. 52-58

- Lyubushin, A. A. and Sobolev, G. A., Multifractal Measures of Synchronization of Microseismic Oscillations in a Minute Range of Periods, *Fiz. Zemli*, 2006, no. 9, pp. 18–28 [*Izv. Phys. Earth (Engl. Transl.)*, 2006, vol. 42, no. 9, pp. 734–744].
- Lyubushin, A. A. Data analysis of geophysical and environmental monitoring systems (*Geophysical and Ecological Monitoring Data Analysis*), Moscow: Nauka, 2007. (Ru)
- Lyubushin, A. A., Microseismic Noise in the Low-Frequency Range (Periods of 1–300 min): Properties and Possible Prognostic Features, *Fiz. Zemli*, 2008, no. 4, pp. 17–34 [*Izv. Phys. Earth (Engl. Transl.)*, 2008, vol. 44, no. 4, pp. 275–290].
- Oynakov E., I. Aleksandrova Seismic characteristics of the earthquake of 10/28/2019 that occurred in the seismogenic region of Vrancea, Romania. *BULGARIAN ACADEMY OF SCIENCES, Problems of Geography*, 2019, Sofia, no 1, pp. 18-28.
- Stehly L., Campillo M., Shapiro N. M. A study of the seismic noise from its long-range correlation-properties // *Journal of Geophysical Research: Solid Earth*. – 2006. – Т. 111. – №. B10
- Samarov A., Taqqu M. S. On the efficiency of the sample mean in long-memory noise // *Journal of Time Series Analysis*. – 1988. – Т. 9. – №. 2. – С. 191-200
- Oynakov E., Fractal characteristics of random fluctuations of seismic records, *Problems of Geography*, 2019, in print

Вариация на параметрите на фоновия сеизмичен шум в етапа на подготовката на силни земетресения в сеизмична зона вранча

Е. Ойнаков, И. Александрова, Д. Солаков

Резюме: Глобалните въздействия на атмосферни и океански процеси, приливни деформации на земната кора, глобалният сеизмичен процес, както и по-слабо проучените процеси в земната кора са свързани с натрупване и бавно разсейване на тектоничната енергия в литосферата. Тези процеси са „участниците“ във формирането на случайния процес, за който изследването с традиционният апарат за спектрален анализ се оказва слабо ефективен.

Използването на фрактален анализ за дешифриране на структурата на сеизмичния шум е достатъчно добра алтернатива. От началото на 90-те години на миналия век методът се използва както в анализа на турбулентността, така и във финансовите и медицинските изследвания на времевите серии.

Разработването на нови методи за прогнозиране на земетресенията, основани на данни от геофизичен и в частност сеизмичен мониторинг, е един от приоритетните цели на науката за Земята. Анализирани са сеизмичните записи на двадесет и три сеизмични станции разположени на територията на Балканския полуостров на разстояния от 1 до 500 км от земетресенията от 23.09.2016 г., 27.12.2016 г. и 28.10.2018 г., с магнитуди повече от 5,5 в сеизмичната зона Вранча. За анализа се използва методът на Любушин за фрактален анализ на скаларните времеви серии.

Научна цел е да се открият общи сигнали, игнориращи „индивидуалното“ поведение на елементите на системите за мониторинг.

Ключови думи: индикатори на земетресения, сеизмичен шум, фрактален анализ на сеизмичен шум

Благодарности: Това проучване е проведено в рамките на Националната научна програма „Млади учени и докторанти“, одобрена с Решение на Министерския съвет № 11 / 17.08.2018 г. и подкрепено от Министерството на образованието и науката (МОН) на България, както и в рамките на Националната научна програма „Опазване на околната среда и намаляване на рисковете от нежелани събития и природни бедствия“, одобрена с Решение на Министерския съвет № 577 / 17.08.2018 г. и подкрепено от Министерството на образованието и науката (МОН) на България (Споразумение № ДО-230 / 06-12-2018 г.).